AIR FORCE REPORT NO.
SAMSO-TR-70-304

AEROSPACE REPORT NO.
TR-0059(9260-01)-1

INTERFEROMETRIC MEASUREMENTS OF THE FAR-INFRARED REFRACTIVE INDEX OF SODIUM FLUORIDE AT LOW TEMPERATURES

Prepared by C. M. Randall
Space Physics Laboratory

70 JUL 15

Laboratory Operations
THE AEROSPACE CORPORATION

Prepared for SPACE AND MISSILE SYSTEMS ORGANIZATION
AIR FORCE SYSTEMS COMMAND
LOS ANGELES AIR FORCE STATION
Los Angeles, California

26

Air Force Report No.
SAMSO-TR-70-304

Aerospace Report No.
TR-0059(9260-01)-1

INTERFEROMETRIC MEASUREMENTS OF THE FAR-INFRARED REFRACTIVE INDEX OF SODIUM FLUORIDE AT LOW TEMPERATURES

Prepared by

C. M. Randall
Space Physics Laboratory

7Ø JUL 15

Laboratory Operations
THE AEROSPACE CORPORATION

Prepared for

SPACE AND MISSILE SYSTEM ORGANIZATION
AIR FORCE SYSTEMS COMMAND
LOS ANGELES AIR FORCE STATION
Los Angeles, California

FOREWORD

This report is published by The Aerospace Corporation, El Segundo, California, under Air Force Contract F04701-70-C-0059.

The author is pleased to acknowledge the contributions of Drs. J. M. Dowling, R. T. Hall, and R. D. Rawcliffe to this work through frequent discussions and the contribution of T. E. Mott to the carrying out of the experimental work.

This report, which documents research carried out from May 1969 through February 1970, was submitted on 16 July 1970 to Lt Gary R. Edwards, SMTAE, for review and approval.

Approved

G. A. Paulikas, Director
Space Physics Laboratory

Publication of this report does not constitute Air Force approval of the report's findings or conclusions. It is published only for the exchange and stimulation of ideas.

Gary R. Edwards, 1st Lt, USAF
Project Officer

ABSTRACT

The refractive index of sodium fluoride at cryogenic temperatures has been determined between 30 and 180 cm^{-1} from channel spectra obtained by Fourier spectroscopy. Fitting the measured refractive index to a Lorentz oscillator model we find a low frequency dielectric constant of 4.70 and a damping parameter varying from 3.3 cm^{-1} at 80K to less than 0.025 cm^{-1} at 10K.

CONTENTS

FIGURES

INTERFEROMETRIC MEASUREMENTS OF THE FAR-INFRARED REFRACTIVE INDEX OF SODIUM FLUORIDE AT LOW TEMPERATURES

Fourier spectroscopy permits the measurement of optical constants in the far-infrared spectral region with an accuracy rivaling that obtained by specialized instruments in other spectral regions. We have applied these techniques to the determination of the far-infrared refractive index of sodium fluoride at low temperatures. First the technique employed is briefly reviewed, the experimental problems of applying the method to low temperature measurements are then discussed, and finally the optical constants obtained for sodium fluoride at liquid nitrogen and liquid helium temperatures are presented.

I. Channel Spectrum Method

The Fourier spectroscopic techniques employed for refractive index measurements may be divided into two classes depending on the location of the sample with respect to the interferometer. If the sample is located within one beam of the interferometer (asymmetric Michelson) both phase and amplitude information are available from which both real and imaginary parts of the refractive index may be determined. If the sample is located outside the interferometer (channel spectrum) the real part of the refractive index can be determined with high accuracy, based on wavenumber measurements, while a less accurate determination of the imaginary part (absorption) is possible based on spectral intensity measurements. Since the two

interfering beams in the Aerospace lamellar grating interferometer (reference 1) are not conveniently spatially separated we employ the channel spectrum method.

The basic sample geometry is shown in figure 1. For light incident on a sample of thickness h at any angle a straightforward and familiar calculation shows the transmittance $T(\nu)$ is:

$$T(\nu) = \tau(\nu)(1 + 2\sum_{\ell=1}^{\infty} \rho^{\ell} \cos \ell\theta) \qquad (1)$$

where ν (= $1/\lambda$) is the wavenumber and the other quantities are related to the complex refractive index $\hat{n} = n + i\,k$ by the following relations (reference 2)

$$\tau(\nu) = 16(n^2 + k^2)\exp(-\alpha h \cos\beta)/\{[(n+1)^2 + k^2]^2(1-\rho^2)\} \qquad (2)$$

$$\rho = [(n-1)^2 + k^2]\exp(-\alpha h \cos\beta)/[(n+1)^2 + k^2] \qquad (3)$$

$$\theta = 4\pi h n \nu \cos\beta + \tan^{-1}[2k/(n^2 + k^2 - 1)] \qquad (4)$$

and $\alpha = 4\pi\nu k$ is the customary absorption constant. β is the angle between the ray and the normal within the sample. The complete transmittance spectrum given by equation consists of a slowly varying average transmittance given by $\tau(\nu)$ modulated by the interference given by the cosine series. The absorption parameter α, may be obtained from the average transmittance by an iterative

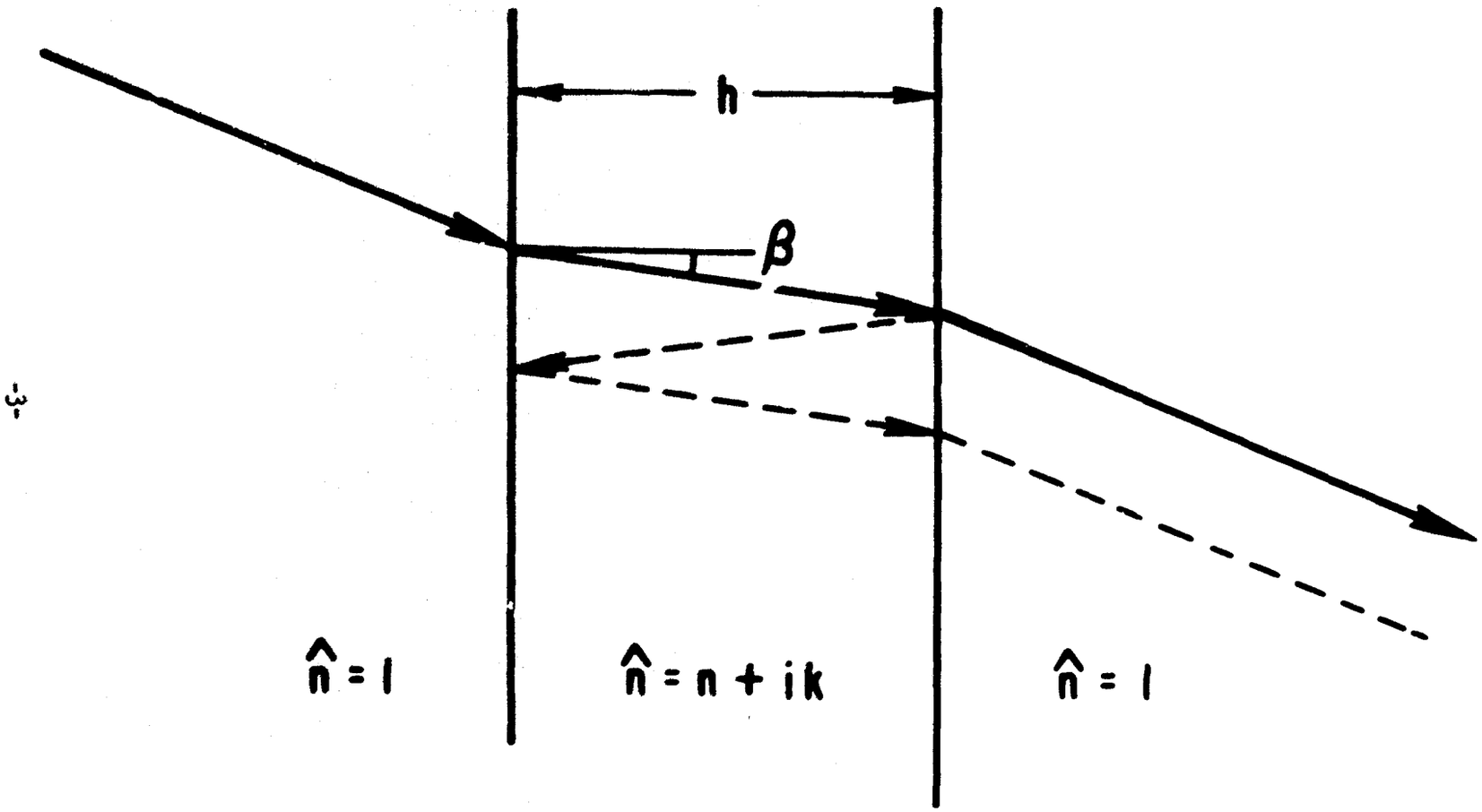

Figure 1 - Channel spectrum sample geometry.

solution of equation 2, once n is known. The modulation will have maxima when the optical thickness is an integral number of half-wavelengths; i.e., when $\theta = 2m\pi$, where m is called the order number. If υ is the wavenumber at which a maximum occurs the real part of the refractive index can be obtained from equation 4.

$$n = m/(2\upsilon h\cos\beta) \tag{5}$$

For the samples studied the imaginary part of the index is small enough to allow the arc-tangent term to be completely ignored.

The assignment of order number, m, must be made with particular care in a material with significant dispersion, such as sodium fluoride. We make this assignment by assuming a functional form for the dependence of n on frequency, then solving equation 5 simultaneously for two different maxima at as low a frequency as possible to obtain a value for the refractive index. This value of n is then used to compute the order number from equation 5. Since the spectral range of our data is well below the characteristic lattice absorption frequence, υ_0, we assume a series expansion of Sellmeier's equation is an adequate function to relate the real refractive index to ϵ_0 and ϵ_∞, the low and high frequency dielectric constants respectively,

$$n = n_0 \left[1 + A(\upsilon/\upsilon_0)^2 \left[1 + B(\upsilon/\upsilon_0)^2 \right] \right] \tag{6}$$

where $A = (\epsilon_0 - \epsilon_\infty)/2\epsilon_0$, and $B = (3\epsilon_0 + \epsilon_\infty)/4\epsilon_0$. A and B may be calculated from crude estimates since they affect only small corrections. $n_0 = \epsilon_0^{\frac{1}{2}}$ will be determined from the simultaneous equation solution. By substituting the value of n_0 back into equation 5 the order number, correct to first order in $(\upsilon / \upsilon_0)^2$, is found after some algebra, in terms of only measurable quantities and A.

$$m = (\Delta m/\Delta \upsilon)\{1 - A(\upsilon/\upsilon_0)^2[2 + 3\phi + \phi^2]\} \qquad (7)$$

where $\Delta\upsilon/\Delta m$ is the frequency change between maxima in the region of the maximum of order m at frequency υ, and $\phi = \Delta\upsilon/\upsilon$. In our worst case the correction term was about 4% and changed the order number by 4. Of course once the order number is correctly assigned at one place in the spectrum is assigned correctly for the entire spectrum.

The form of equation 1 as a cosine series emphasizes the advantage of taking data for this method by means of an interferometer which Fourier cosine transforms equation 1 so that the coefficients of the various terms become physically separated in "signatures" occuring at regularly spaced intervals in interferometer optical path difference. We take advantage of this by obtaining data away from zero path difference in a manner to maximize the signal to noise ratio in the signatures. This optimizes the precision of the wavenumber determination in the modulation of the transmittance spectrum. The portion of the

interferogram about zero path difference is determined in a manner to optimize the amplitude accuracy of the spectrum. The average transmittance is determined from this amplitude spectrum appropriately corrected. Room temperature refractive index measurements by these methods have already been completed for a number of materials. (references 2 and 3)

II. Low Temperature Measurements

We have chosen to extend these measurements to low temperatures because of the increased insight into the mechanisms for optical constant change in solids and because many potential uses of materials in the far-infrared will be in cooled systems.

Because of the convenience of maintaining only one cryostat many investigators place their samples in the light pipe leading from the interferometer to the cooled detector. We have chosen the more complicated route of a separate sample dewar to permit more careful definition of the angles with which radiation strikes the sample and to allow the sample temperature to be varied independently while the detector is maintained at its optimum operating temperature.

With a separate dewar it is important that differences in emission between a cold sample and its warm surroundings are not confused with changes in transmittance. Figure 2, which is a schematic diagram of the sample optics of the Aerospace interferometer, illustrates how this confusion may arise. In an absorbing spectral region the transmittance of the sample is low and the emissivity high so the detector sees the difference between a 300 K object in the lower beam

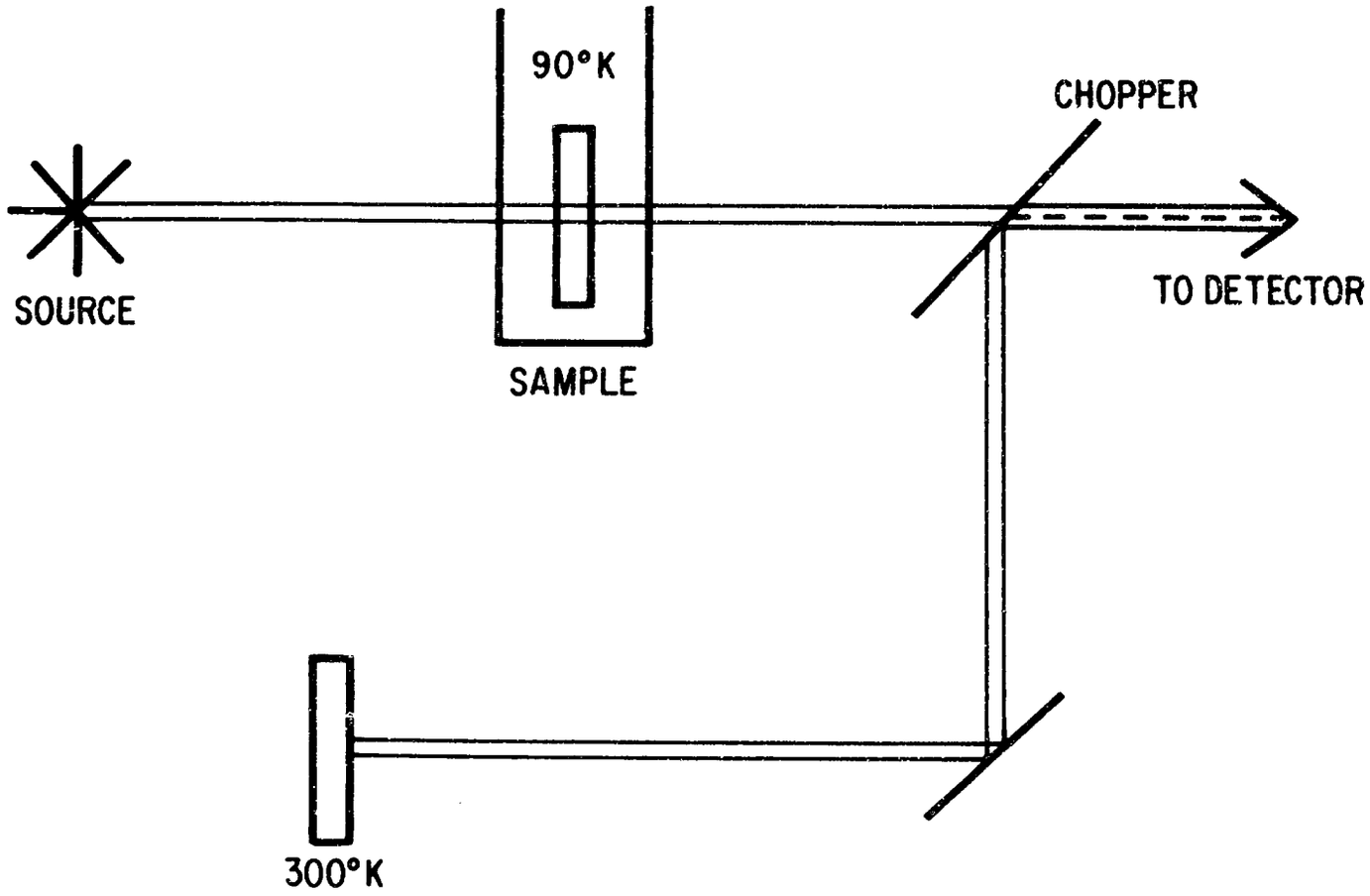

Figure 2 - Schematic diagram of the Aerospace lamellar grating interferometer sample optics arranged for a single beam run.

and a 90 K object in the upper beam. The effect is to superimpose on the transmittance spectrum a spectrum of the difference in emission. Figure 3 is such a difference of emission spectrum comparing polyethlyene at liquid nitrogen temperature with black anodized aluminum at room temperature. No source illuminates either material. Over most of the spectral region the detector sees through the quite transparent polyethylene to the room temperature surroundings and so the difference spectral intensity is not large. However in the polyethylene absorption band at 70 cm^{-1} the detector views an object at liquid nitrogen temperature. The room temperature aluminum emits more energy that the polyethylene so the difference spectral intensity increases significantly. This occurs at just the places in the spectrum where there is usually the most interest in obtaining accurate measurements of transmittance from the composite spectrum.

These problems may be avoided by chopping the radiation before it passes through the cold sample. This has required the installation of a new chopper in the Aerospace interferometer. It is shown, along with the dewar in figure 4. This chopper is driven by a stepping motor which allows a variation in chopping frequency from zero up to about 25 Hz. The samples are mounted behind the window in the dewar tail on a high conductivity copper cold finger.

III. Sodium Fluoride Results

Sodium fluoride was chosen for study for several reasons. There is considerable theoretical interest in the simple cubic

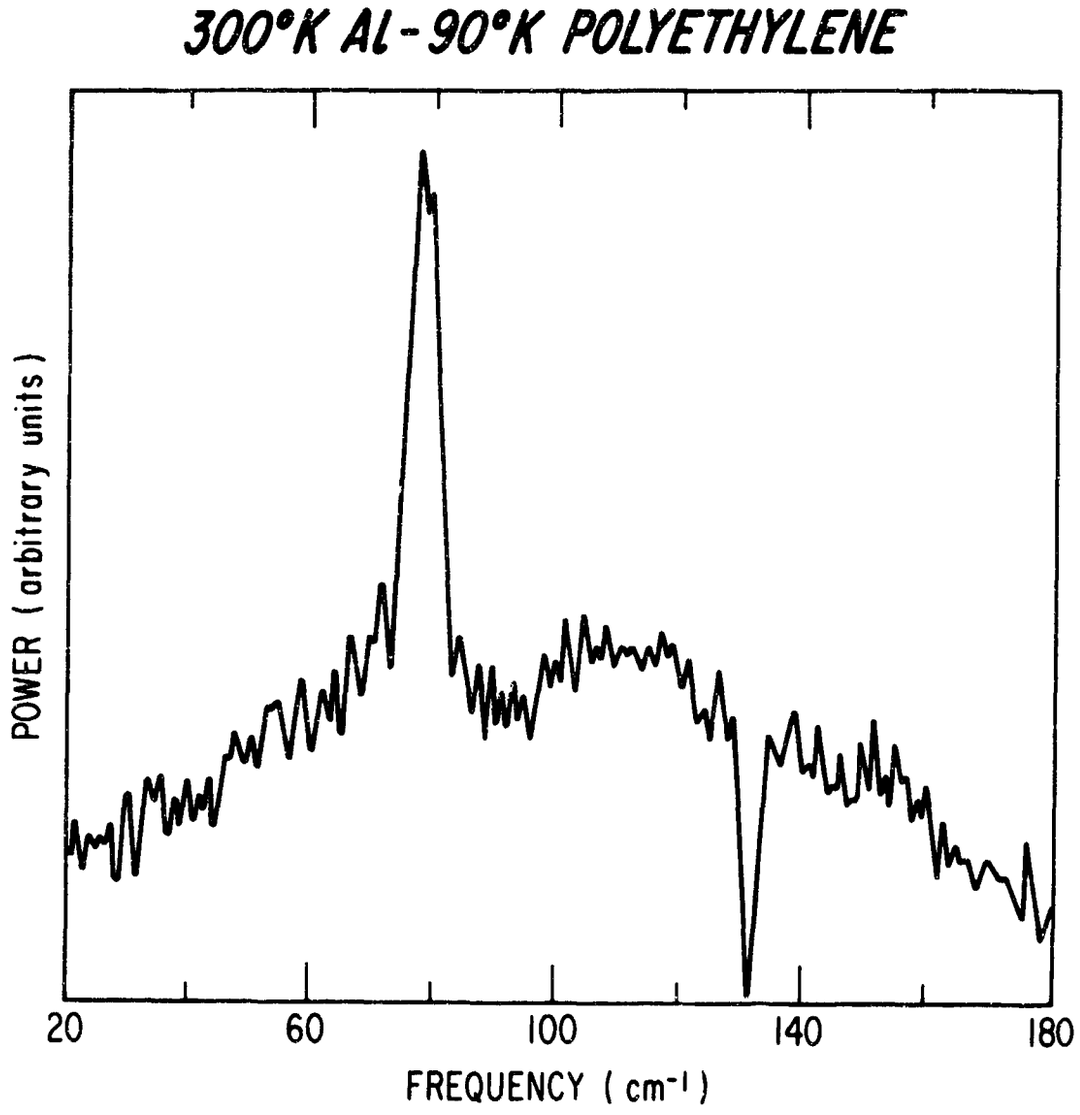

Figure 3 - Spectrum due to the difference in emission between a black anodized aluminum sheet at room temperature and polyethylene at liquid nitrogen temperature. The detecting electronics are adjusted so that increasing emission from the aluminum gives a positive signal. The absorption at 130 cm^{-1} is due to a cold crystal quartz window in the detector cryostat.

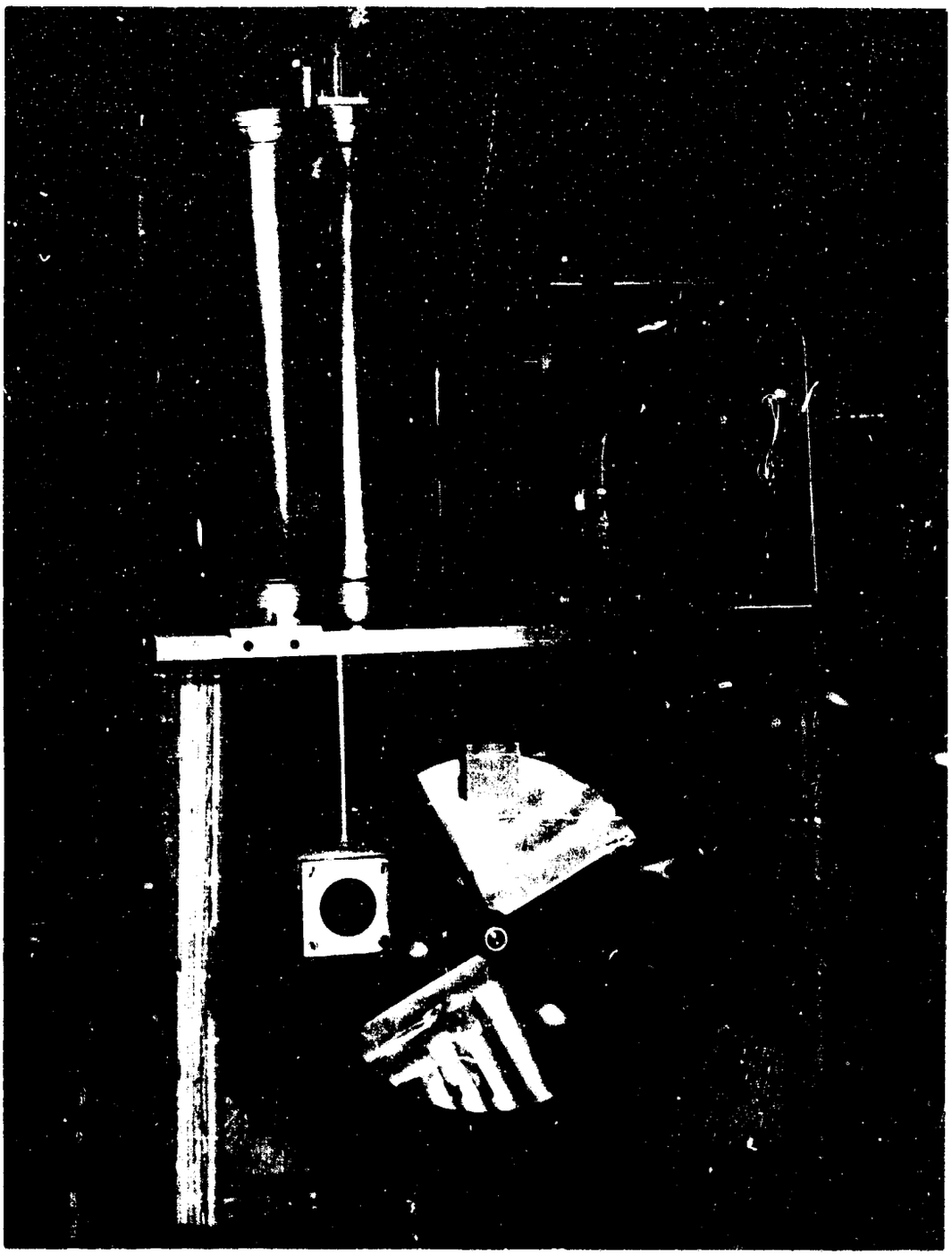

Figure 4 - Dewar and chopper for the Aerospace lamellar grating interferometer.

ionic crystals. The alkali halides show a super-transparency at low temperatures indicating marked change in their optical parameters. Also there is some diversity in the values quoted for the low frequency dielectric constant (reference 4). We have obtained interferograms of the channel spectrum and the average transmittance spectrum of a 0.5639 cm thick crystal of sodium fluoride at liquid nitrogen and liquid helium temperatures.

Because of the dispersion in NaF the signatures in the interferogram which gives the channel spectrum are very asymmetric. This is emphasized in figure 5 which shows portions of the NaF signature and for comparison the signature of a sample of very low dispersion silicon.

Shown in figure 6 is the refractive index obtained by the means outlined above from the Fourier cosine transform of interferograms such as that shown in figure 5. To determine the low frequency dielectric constant ϵ_0, more accurately we have least squares fit the real refractive index data to a Lorentz oscillator model for which the complex dielectric constant $\epsilon = (\hat{n})^2 = (n + ik)^2$ is:

$$\epsilon = \epsilon_\infty + (\epsilon_0 - \epsilon_\infty)/\left[1 - (\nu/\nu_0)^2 + i(\gamma\nu/\nu_0^2)\right] \qquad (8)$$

where ϵ_∞ is the dielectric constant at frequencies far above the characteristic frequence, ν_0, and γ is a damping constant. The values chosen for the constants are; $\epsilon_\infty = 1.755$ (reference 5) and

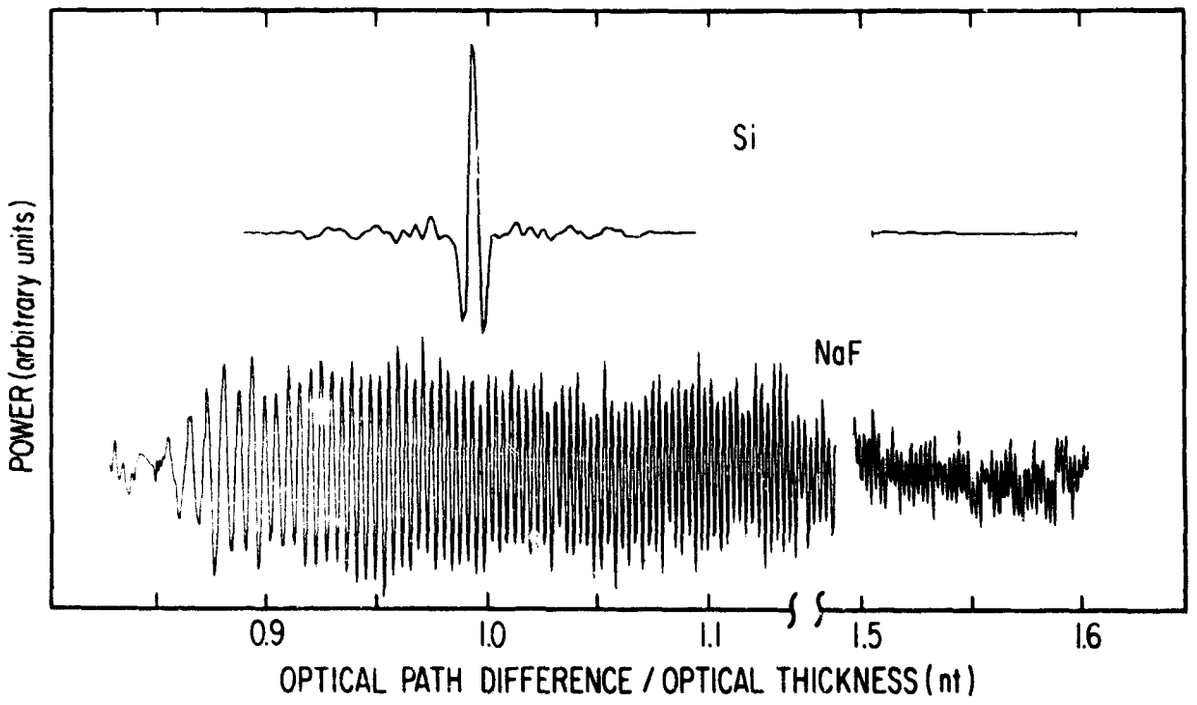

Figure 5 - Channel spectrum signature of sodium fluoride at liquid helium temperature. The signature of a silicon sample is shown in comparison.

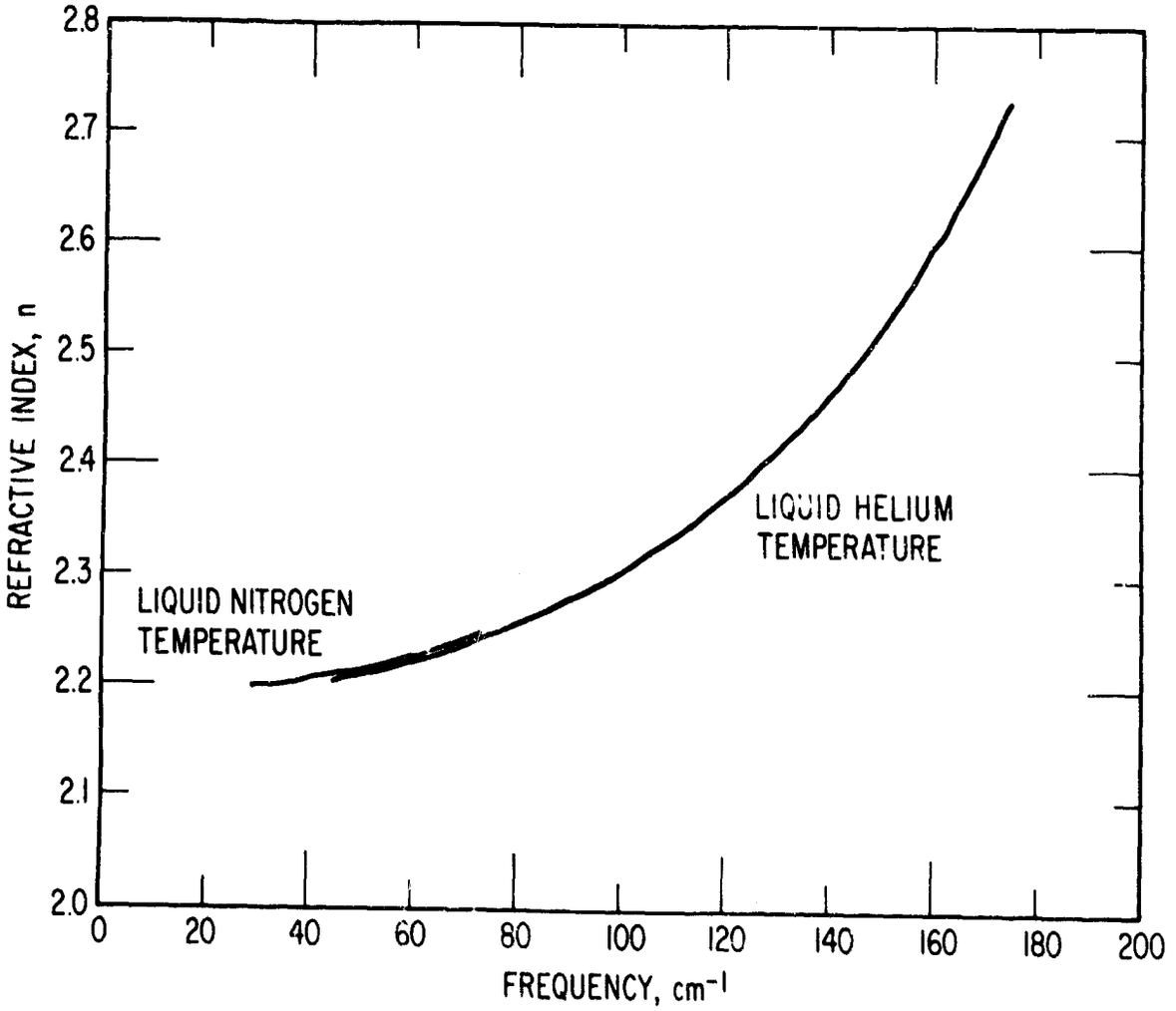

Figure 6 - Real part of the refractive index of sodium fluoride at liquid nitrogen and liquid helium temperatures.

$\nu_0 = 246$ cm^{-1} (reference 6). γ is obtained from the average transmittance spectrum analysis discussed below. Only ϵ_0 is allowed to vary. The best fit value is 4.70 ± 0.02. We do not observe any significant change with temperature in the real part of the refractive index in the spectral region where data from both liquid nitrogen and liquid helium temperatures are available.

There is however, a significant decrease in the imaginary part of the refractive index with temperature as indicated by the temperature dependence of the average transmittance shown in figure 7. These curves were made by transforming only the portion of a single beam interferogram near zero path difference and correcting for source spectral variation, window transmittance, and sensitivity changes of the instrument to obtain the average transmittance $\tau(\nu)$. From these transmittance curves, the absorption $\alpha = 4\pi\nu k$ was found by means of equation 2 and the measured real refractive index. The resulting absorption parameters are shown in figure 8.

To characterize this change in absorption with temperature by a single parameter we have again employed the Lorentz oscillator in a least squares fit to the measured absorptions, varying only γ. The value chosen for ϵ_0 was 4.70 from the real index measurements and the other constants were the same as those used in the real index calculations. For the liquid nitrogen temperature data this procedure was straightforward and a value of 3.3 cm^{-1} was obtained for γ. For comparison the calculated absorption for a Lorentz oscillator with this damping is shown on figure 8. At liquid helium temperature the absorption is so small that the noise in the limited

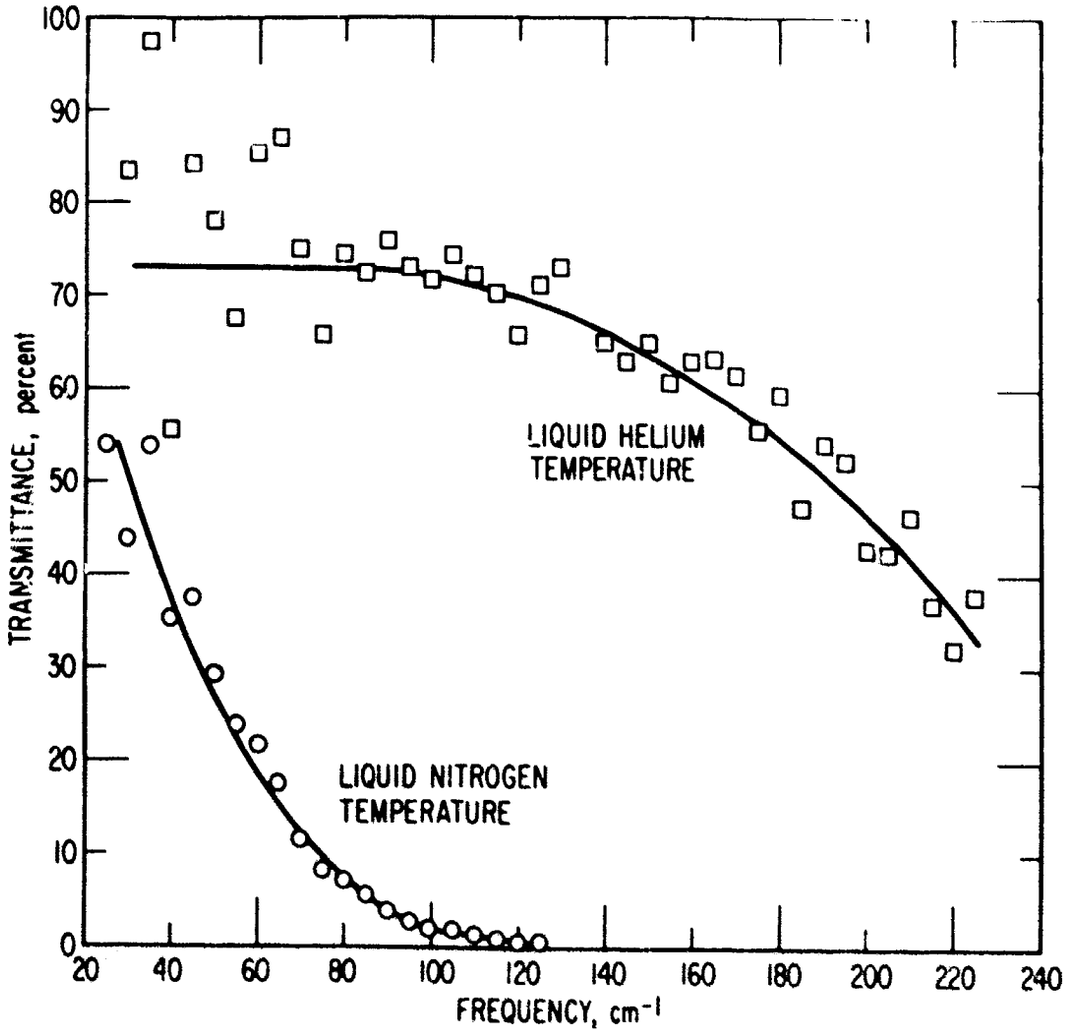

Figure 7 - Far-infrared transmittance of sodium fluoride at low temperatures. O liquid nitrogen temperature, □ liquid helium temperature.

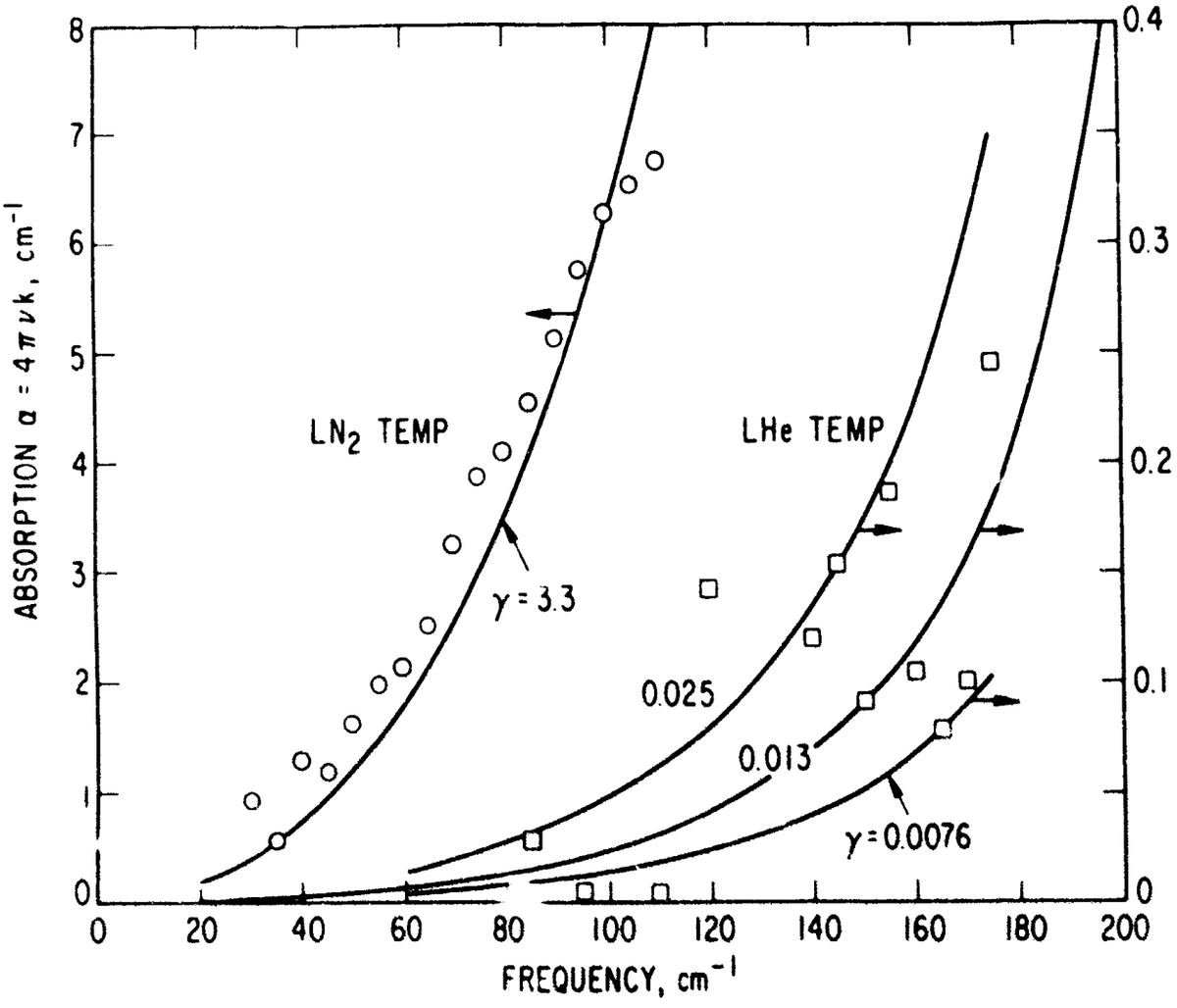

Figure 8 - Absorption $= 4\pi\nu k$, for sodium fluoride at low temperature. ○ liquid nitrogen temperature, □ liquid helium temperature. The smooth curves are absorptions calculated for a Lorentz oscillator model dielectric with $\epsilon_0 = 4.70$, $\epsilon_\infty = 1.755$ and $\nu_0 = 246.0$ cm^{-1} and the values of γ in units of cm^{-1} shown on the figure.

data available obscures any clear trend in the absorption. We have therefore plotted in figure 8 the absorption for several values of γ which give absorption parameters which bracket most of the experimental points.

Values of the damping constant at intermediate temperatures will be of interest to differentiate between various mechanisms suggested for the absorption of infrared radiation by the alkali halides, since different mechanisms have somewhat different absorptance temperature dependence. We are presently modifying our dewar for variable temperature operation so this functional dependence on temperature may be investigated.

REFERENCES

1. R. T. Hall, D. Vrabec, and J. M. Dowling, Appl. Opt., 5, 1147 (1966).

2. C. M. Randall and R. D. Rawcliffe, Appl. Opt., 6, 1889 (1967).

3. C. M. Randall and R. D. Rawcliffe, Appl. Opt., 7, 213 (1968).

4. W. J. L. Buyers, Phys. Rev., 153, 923 (1967).

5. American Institute of Physics Handbook, Second Edition, D. E. Gray ed. McGraw Hill, New York (1963).

6. C. M. Randall, R. M. Fuller, and D. J. Montgomery, Solid State Commun, 2, 273 (1964).

UNCLASSIFIED

Security Classification

DOCUMENT CONTROL DATA - R & D

(Security classification of title, body of abstract and indexing annotation must be entered when the overall report is classified)

1. ORIGINATING ACTIVITY *(Corporate author)*

The Aerospace Corporation
El Segundo, California

2a. REPORT SECURITY CLASSIFICATION
Unclassified

2b. GROUP

3. REPORT TITLE

INTERFEROMETRIC MEASUREMENTS OF THE FAR-INFRARED REFRACTIVE INDEX OF SODIUM FLUORIDE AT LOW TEMPERATURES

4. DESCRIPTIVE NOTES *(Type of report and inclusive dates)*

5. AUTHOR(S) *(First name, middle initial, last name)*

Charles M. Randall

6. REPORT DATE	7a. TOTAL NO. OF PAGES	7b. NO. OF REFS
70 JUL 15	22	6

8a. CONTRACT OR GRANT NO.	9a. ORIGINATOR'S REPORT NUMBER(S)
F04701-70-C-0059	TR-0059(9260-01)-1
b. PROJECT NO.	
c.	9b. OTHER REPORT NO(S) *(Any other numbers that may be assigned this report)* SAMSO-TR-70-304
d.	

10. DISTRIBUTION STATEMENT

This document has been approved for public release and sale; its distribution is unlimited.

11. SUPPLEMENTARY NOTES	12. SPONSORING MILITARY ACTIVITY
	Space and Missiles Systems Organization Air Force Systems Command Los Angeles, California

13. ABSTRACT

The refractive index of sodium fluoride at cryogenic temperatures has been determined between 30 and 180 cm^{-1} from channel spectra obtained by Fourier spectroscopy. Fitting the measured refractive index to a Lorentz oscillator model we find a low frequency dielectric constant of 4.70 and a damping parameter varying from 3.3/cm^{-1} at 80K to less than 0.025/cm^{-1} at 10K.

DD FORM 1473 (FACSIMILE)

UNCLASSIFIED

Security Classification

14

KEY WORDS

Far-Infrared
Interferometry
Refractive Index
Sodium Fluoride

Distribution Statement (Continued)

Abstract (Continued)